

A Technique for Making Nuclear Fusion in Solids_Diversification

R. Wayte

29 Audley Way, Ascot, SL5 8EE, England, UK.

Email: dr.wayte@audleyscientific.com

Abstract: A technique is demonstrated for making nuclear fusion by shearing or electrically-igniting compressed mixtures of numerous hydride+catalyst powders. Controlled explosions have been generated which are stronger than exothermic chemical reactions for the materials.

Keywords: Nuclear fusion, Solid state

Research article: 26 March 2026

1 Introduction

Nuclear fusion needs to be developed in order to reduce global-warming, see original articles [1], [2]. Inertial confinement fusion, employing a projectile to impact a nuclear fuel target, might become the most economical method for energy production if these newfound fuels were substituted for DT, [3]. Other machines using lasers could achieve real success with these fuels.

In the two previous articles, it was demonstrated how nuclear fusion could be generated by mechanically shearing specific mixtures of deuteride, hydride and catalyst powders. Alternatively, an ionising electric current could be passed through the compressed mixture without shearing. In this article, the specific mixtures used previously will be diversified by substituting many other elements which will confirm the broad reality of this technique.

2 Experimental methods

A reproducible effect has been found with a view to useful energy generation. Experiments were conducted inside a transparent box and were regarded as successful when the ignition produced a bright flash and loud explosion with smoke; while the hardened steel anvils were pitted, cracked or broken, and the acrylic cell was totally fractured and fragmented.

2.1 Fuel preparation.

The first variation of the fusion fuel used in reference [2] ($\text{LiAlH}_4 + \text{B}_4\text{C} + \text{Zn}$) was made by mixing lithium aluminium hydride powder LiAlH_4 (>95%)(LAH) with zirconium carbide powder ZrC (>95%) and metallic zinc powder Zn (>95%); [DR, private communication]. Particle sizes of the powders were in the range $<50\mu\text{m}$, while the weight proportions were around (1:1:1). These values were not critical here but optimisation for a given project would be beneficial.

This fuel variation involved exchanging one hard material B_4C (Vickers 38GPa) for another ZrC (Vickers 25GPa). Zinc powder appears to be functioning as electron provider for Coulomb screening and it may be exchanged for other metals. Further variations will follow these principles.

Given the success of ZrC , some hard zirconium nitride ZrN powder (Vickers 23GPa) was substituted and found to be equally effective. Another well-known hard material tungsten carbide WC powder (Vickers 24GPa) was then substituted with ($\text{Zn} + \text{LAH}$), and proved very successful; likewise, for silicon carbide SiC powder (Vickers 26GPa).

Other metals were then substituted for the original electron provider zinc powder. Iron powder with ($\text{B}_4\text{C} + \text{LAH}$) proved successful; as did aluminium powder and tin powder. Oddly, amorphous boron powder (Vickers 45GPa) performed quite well.

Then the hard component and metallic component were both varied at the same time: for example, ($\text{WC} + \text{Ta} + \text{LAH}$), ($\text{WC} + \text{Pb} + \text{LAH}$), ($\text{WC} + \text{Bi} + \text{LAH}$), and ($\text{WC} + \text{W} + \text{LAH}$) were successful. Remarkably, boron carbide, tungsten carbide and amorphous boron were found to function both as the hard component and electron provider, such that ($\text{B}_4\text{C} + \text{LAH}$), ($\text{WC} + \text{LAH}$) without metal proved fruitful, but ($\text{B} + \text{LAH}$) was successful only for shearing. In future, the light-weight mixture ($\text{B}_4\text{C} + \text{LiBH}_4$) or ($\text{B}_4\text{C} + \text{LiBD}_4$) may be ideal for propulsion.

Finally, a variation of the earliest work [1] was tried: therein, the mixture for shear-ignition only was ($\text{Mn} + \text{P} + \text{CaD}_2/\text{CaH}_2$). Here, LAH has provided hydrogen while manganese+sulphur was the catalyst, ($\text{Mn} + \text{S} + \text{LAH}$); [JU, private communication]. This powder mixture was very easy to ignite by shearing; but not electrically. Sulphur appears to be performing as the screening-component because the next variation ($\text{B}_4\text{C} + \text{S} + \text{LAH}$) was also easy to ignite by shearing, and electrically due to B_4C being

semi-conductive. After these four experiments, more manganese was added to increase conduction for (5Mn+S+LAH) and get effective electrical-ignition.

Probably, these examples of hard component and electron provider could be expanded to include: AlB_2 , MoC, NbC, SiN, TaC, TiB_2 , TiC, TiN, VC, mixed with a wide choice of metals. A full range of experiments on a real power-plant will reveal the optimum fuel mixture for energy generation. Lithium aluminium hydride has been used throughout for convenience here but a deuteride such as LiBD_4 might be beneficial in other projects. It is fortunate that all these chemicals are readily available and tritium is not involved.

2.2 Shear-ignition fusion experiments.

In these experiments, typically 80mg of the fuel powder was put in a compression cell consisting of two hardened chrome steel roller bearings aligned as the anvils in an acrylic block, see Figure 1. When such a primed cell was subjected to compression in a hydraulic-press (1 - 3)tonne, it exploded powerfully. This was not a simple bursting process because the resulting steel anvils show multiple pitting, cracks and breakages, while acrylic fragments have wedge forms and the larger pieces contain multiple fractures emanating from the central fuel position. Figures 2a–d show examples of steel anvils broken by the extreme fusion pressure acting on a small area of the anvil face, producing a wedge form. No known chemical reaction for these mixtures could do this.

It is deduced that the compression causes shear-ignition within the fuel such that hot-spots in the shear-plane liberate hydrogen from the LAH. Some of this hydrogen is trapped within surface interstices in the hard particles (B_4C , etc.) of the two shearing faces, where it is immediately shear-ionised. Proton-proton fusion may then occur, subject to Coulomb screening in the pressurised hot-spot plasma, aided by concentrations of electrons near metal particles (Zn, etc.). This fusion process ceases as soon as the pressure is relieved by fractures, so runaway is impossible. There is no conflagration of the whole fuel, so much of it is blown out of the fragmenting cell unburnt. This means it is not a chemical detonation process as found in high explosives.

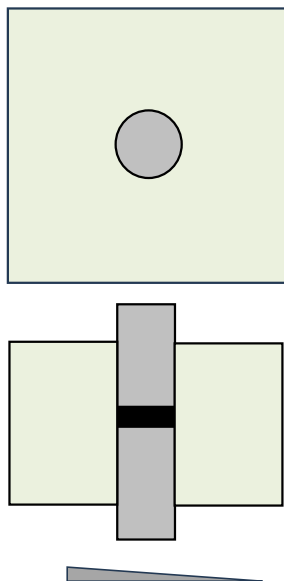


Fig.1. Compression cell design showing fuel between steel anvils (\varnothing 6mm x l 20mm) aligned in an acrylic block (35mm x 35mm x 20mm). A thin steel wedge underneath helps induce shearing.



Fig. 2a Experiment 228 ($B_4C+Zn+LAH$) An anvil shattered due to the small wedge shown which was formed under extreme pressure. The opposing anvil (not shown) was pitted but not broken.



Fig. 2b Experiment 225 ($\text{ZrC}+\text{Zn}+\text{LAH}$) An anvil shattered due to the small wedge shown. The opposing anvil was pitted but not broken.



Fig. 2c Experiment 223 ($\text{ZrN}+\text{Zn}+\text{LAH}$) An anvil shattered due to the small wedge shown. The opposing anvil shows damage on the contact face.



Fig. 2d Experiment 249 (WC+LAH) One anvil shattered due to the shock wave started by the small wedge shown. The opposing anvil shows damage on the contact face. The acrylic cell was shattered by the shock-wave.

2.3 Electrical-ignition fusion experiments.

Experiments were done employing electrical-ignition for compressed cells as in Figure 1. These increased overall knowledge of the phenomenon even if the impact method [3] is chosen for energy production. To ignite the fuel, a high current pulse was applied from a $1350\mu\text{F}$ electrolytic capacitor (C) charged to 650volts (V). The cell would explode, producing acrylic debris similar to the shear experiments with the steel anvils pitted and cracked.

The explosion strength and speed depended on the fuel type, the compression load, and the conduction path through the fuel. Load force has been monitored by means of a Tekscan Force Sensor A502 placed under the cell, which was calibrated and proved to be hardy.

During the ignition, the applied capacitor voltage was monitored and found to be especially informative for medium-compression force, as shown in Figures 3a-k. The discharge current at the beginning may be greater than 10,000amp ($I = -C \text{ dV/dt}$), as if the ionised fuel is a conductive plasma, but then the current is often attenuated or

even reversed by the strong explosion pushing electrons into the capacitor while the fuel plasma is being blown out of the cell. The ignition characteristics illustrated below vary greatly for eleven different mixtures, so there will be a need for optimisation when choosing the best fuel and ICF machine operating conditions for energy generation.

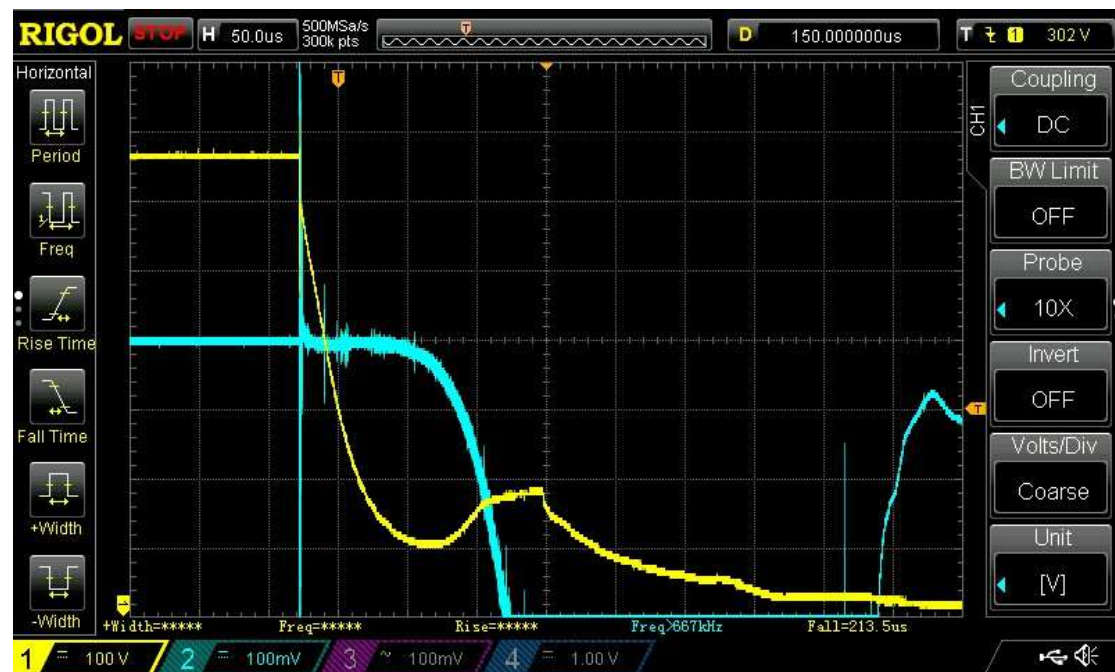


Fig. 3a. Experiment 218 ($B_4C+Zn+LAH$) Yellow trace:- For ignition at medium-compression force, the applied voltage on the capacitor shows that after $90\mu s$ the discharge is halted and reversed by a flow of charge from the plasma forced back into the capacitor over a period of $100\mu s$; then the discharge continues to zero. Turquoise trace:- Compression load measured during the ignition starts at 0.8tonne then shows a large glitch of crosstalk distortion then a small but real increase due to the explosion. The following deep fall lasts while the fuel plasma is blown out of the fragmenting cell over $250\mu s$, then weaker loading is re-established as the anvils make contact together without any fuel or acrylic cell. NB:-The bottom of the screen is at a load offset of 0.15tonne, not zero.

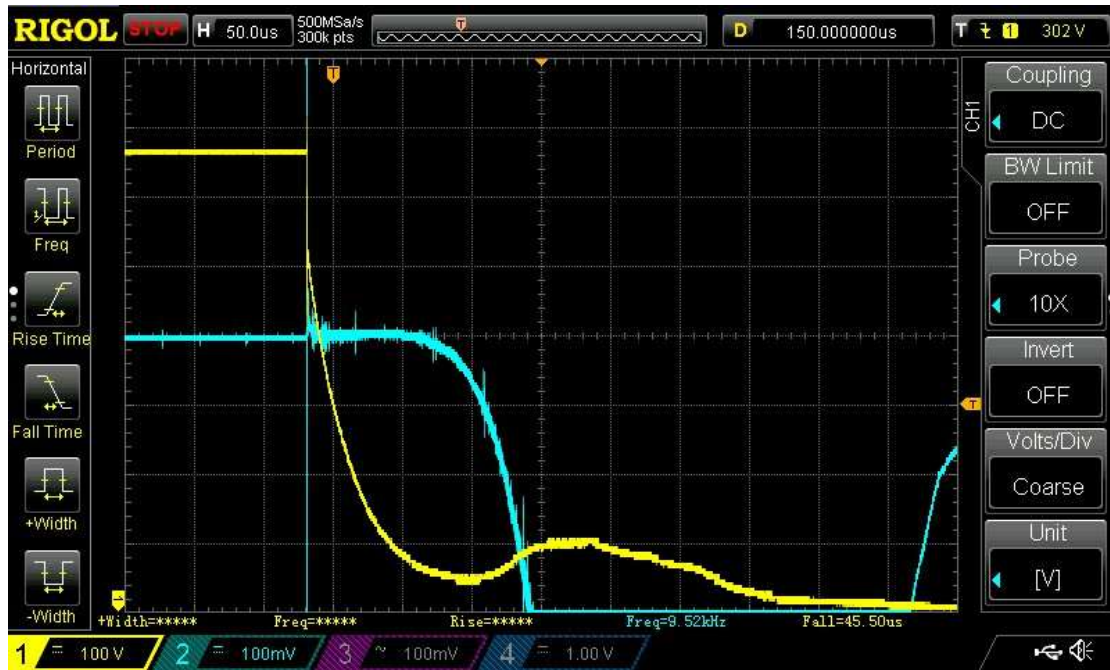


Fig. 3b. Experiment 219 (ZrC+Zn+LAH) Yellow trace:- For ignition at medium-compression force, the applied voltage on the capacitor shows that after $100\mu\text{s}$ the discharge is counteracted by a flow of charge from the plasma forced back into the capacitor over a period of $200\mu\text{s}$. Turquoise trace:- Compression load measured during the ignition.

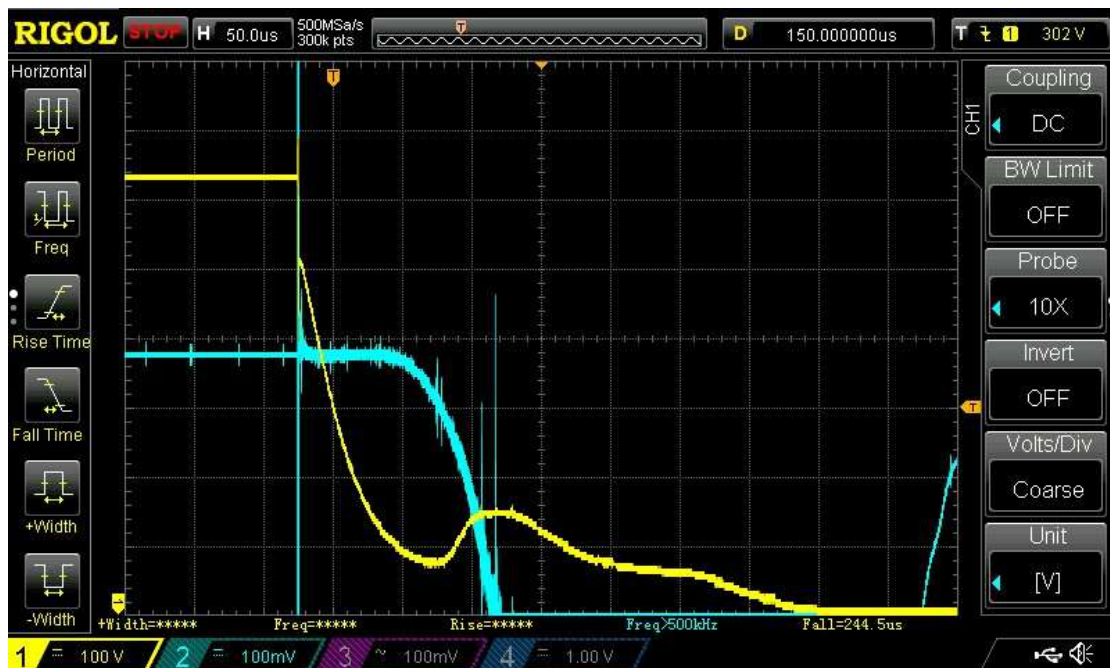


Fig. 3c. Experiment 220 (ZrN+Zn+LAH) Yellow trace:- For ignition at medium-compression force, the applied voltage on the capacitor shows that after $100\mu\text{s}$ the discharge is counteracted by a flow of charge from the plasma back into the capacitor over a period of $150\mu\text{s}$. Turquoise trace:- Compression load measured during the ignition.



Fig. 3d. Experiment 230 (WC+Zn+LAH) Yellow trace:- For ignition at medium-compression force, the applied voltage on the capacitor shows that after $70\mu\text{s}$ the discharge is counteracted by a flow of charge from the plasma back into the capacitor over a period of $50\mu\text{s}$. Turquoise trace:- Compression load measured during the ignition.



Fig. 3e. Experiment 234 (SiC+Zn+LAH) Yellow trace:- For ignition at medium-compression force, the applied voltage on the capacitor shows that after $50\mu\text{s}$ the rapid discharge is counteracted by a flow of charge from the plasma back into the capacitor over a period of $50\mu\text{s}$. Turquoise trace:- Compression load measured during the ignition.

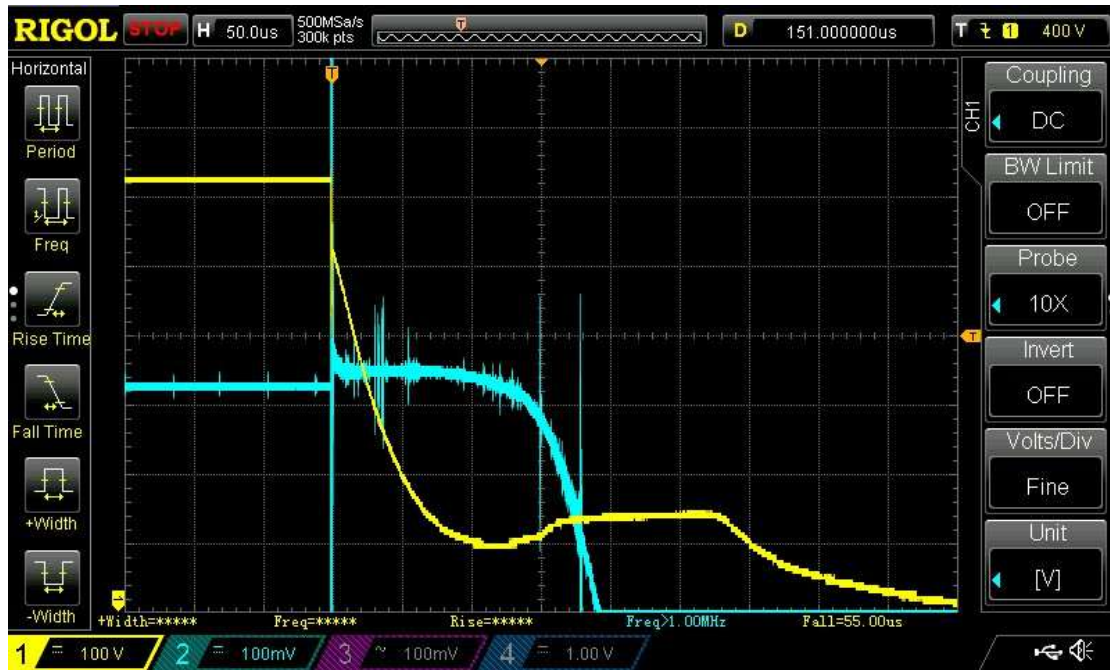


Fig. 3f. Experiment 237 ($B_4C+Fe+LAH$) Yellow trace:- For ignition at medium-compression force, the applied voltage on the capacitor shows that after $120\mu s$ the discharge is counteracted by a flow of charge from the plasma back into the capacitor over a period of $200\mu s$. Turquoise trace:- Compression load measured during the ignition.



Fig. 3g. Experiment 242 ($B_4C+Al+LAH$) Yellow trace:- For ignition at medium-compression force, the applied voltage on the capacitor shows that after $140\mu s$ the rapid discharge is counteracted by a flow of charge from the plasma back into the capacitor over a period of $70\mu s$. Turquoise trace:- Compression load measured during the ignition.

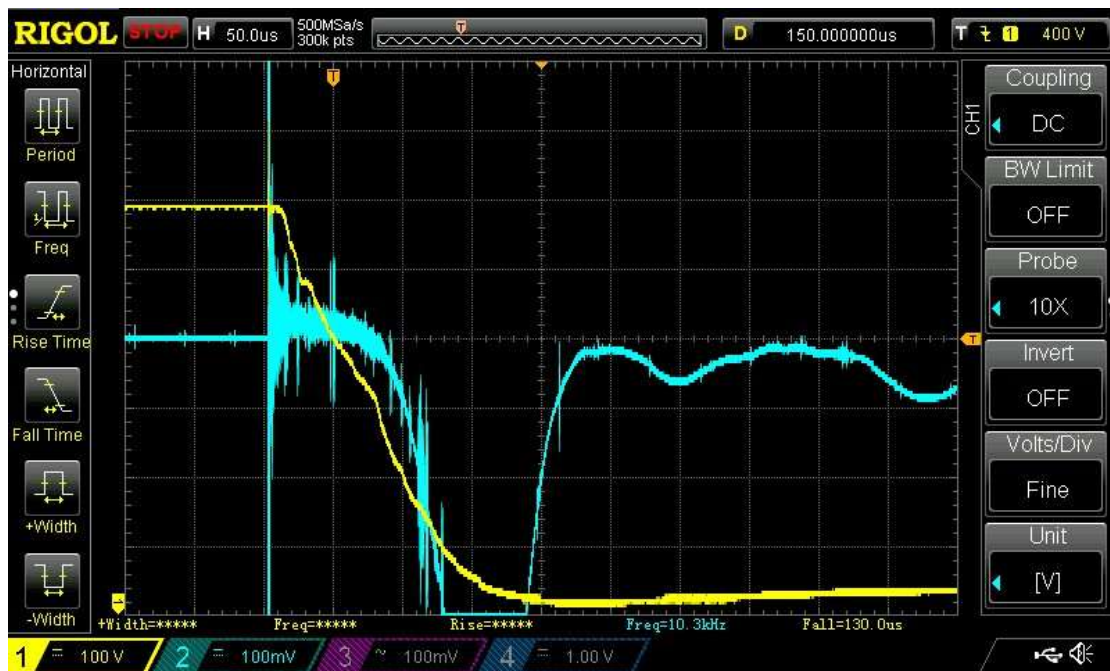


Fig. 3h. Experiment 270 ($B_4C+B+LAH$) Yellow trace:- For ignition at medium-compression force, the applied voltage on the capacitor shows that after $20\mu s$ the discharge rate is decreased, weakly opposed by the plasma over a period of $80\mu s$. Turquoise trace:- Compression load measured during the ignition.

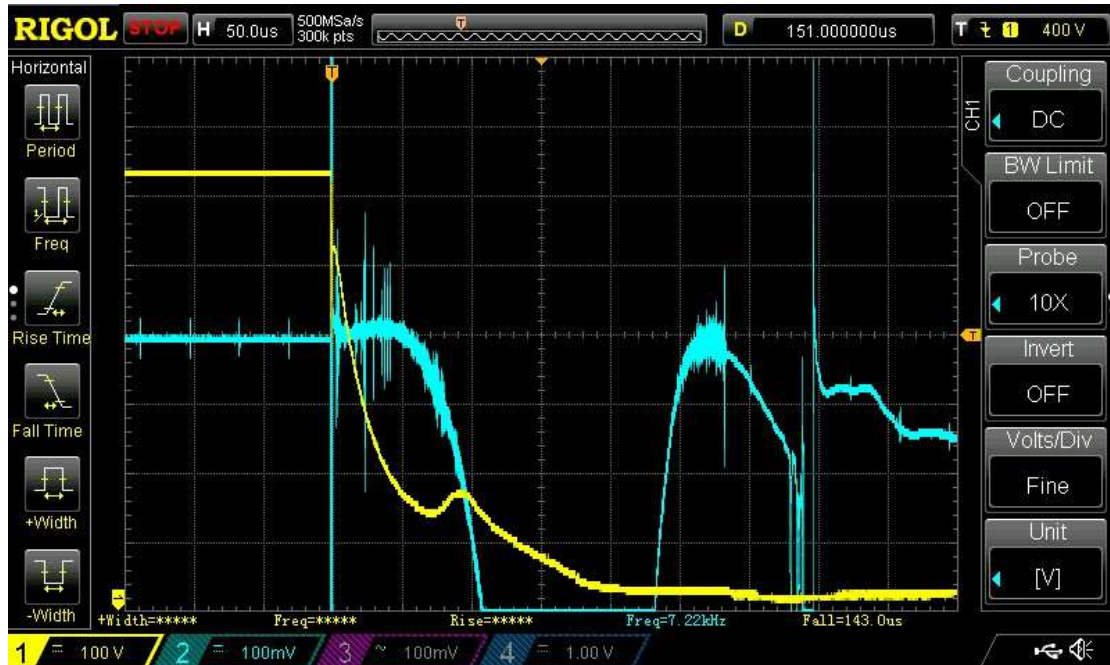


Fig. 3i. Experiment 240 ($WC+Bi+LAH$) Yellow trace:- For ignition at medium-compression force, the applied voltage on the capacitor shows that after $80\mu s$ the discharge is counteracted by a flow of charge from the plasma back into the capacitor over a period of $50\mu s$. Turquoise trace:- Compression load measured during the ignition. The large glitch was due to a faulty contact.

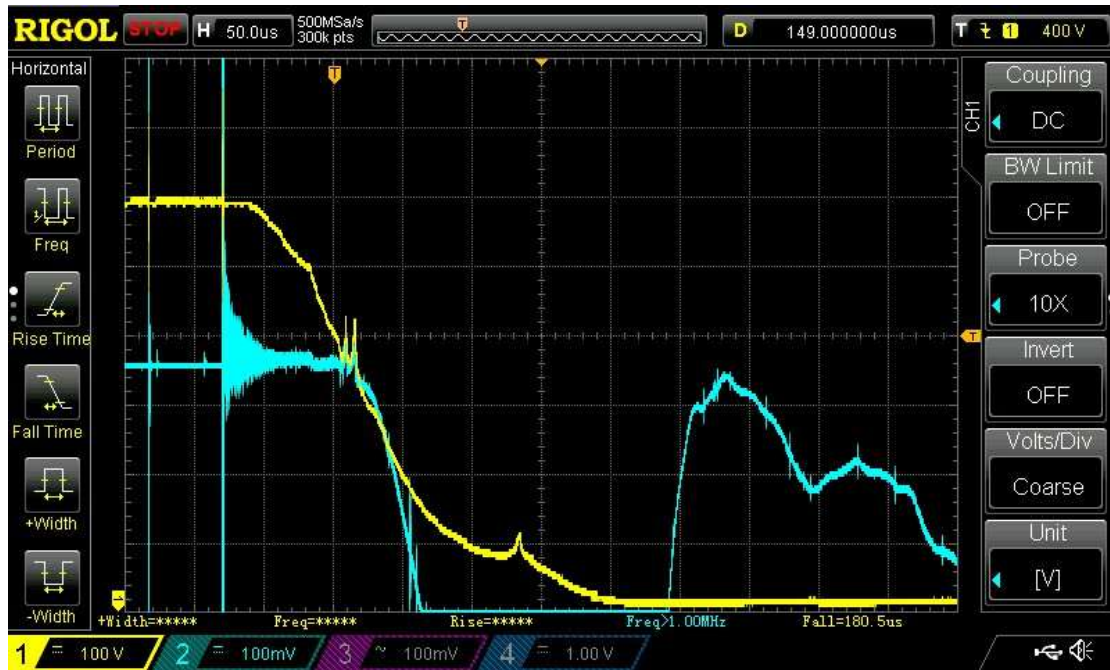


Fig. 3j. Experiment 233 (WC+LAH) Yellow trace:- For ignition at medium-compression force, the applied voltage on the capacitor shows that the discharge is comparatively slow then counteracted by a limited flow of charge from the plasma back into the capacitor over a period of $10\mu\text{s}$ only, then again at $200\mu\text{s}$. Turquoise trace:- Compression load measured during the ignition.

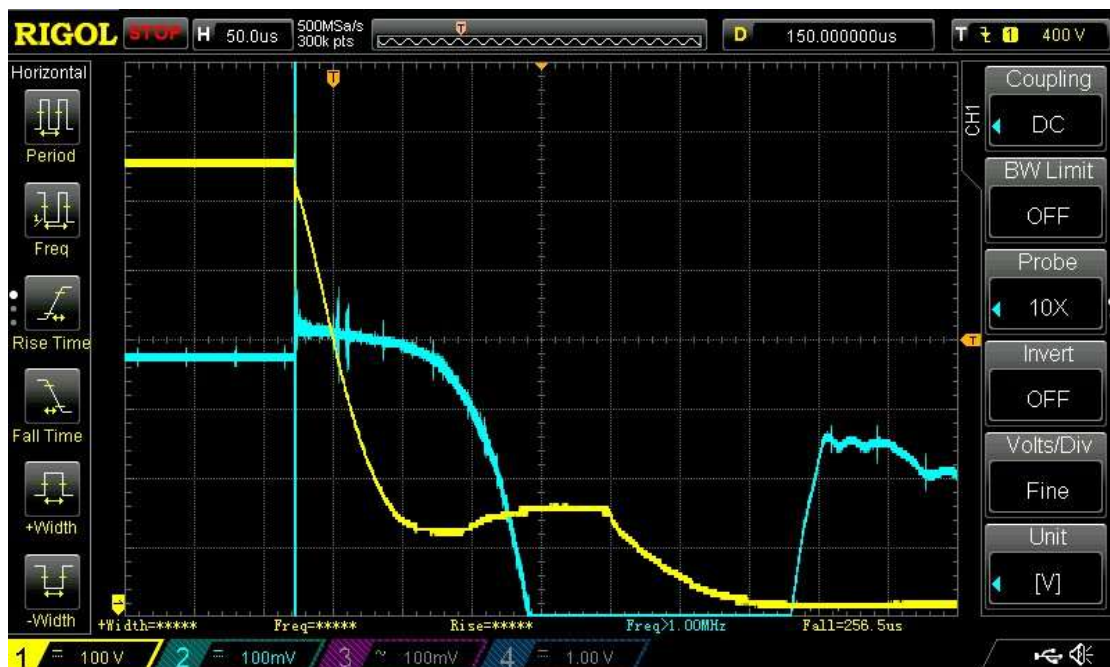


Fig. 3k. Experiment 273 (B_4C +LAH) Yellow trace:- For ignition at medium-compression force, the applied voltage on the capacitor shows that the discharge is comparatively slow (cf. Fig.3a) then counteracted by a flow of charge from the plasma back into the capacitor over a period of $150\mu\text{s}$. Turquoise trace:- Compression load measured during the ignition.

3 Proposed chemical processes

Explosions have been generated, which are stronger than exothermic chemical reactions for the materials. To explain these, it is proposed that nuclear reactions must occur within the fuel when it is compressed then forcefully ionised electrically or by shearing. First, hydrogen is liberated from the lithium aluminium hydride and trapped within interstices in zirconium carbide and zinc particles, for example. Here, the atoms are dynamically constrained then ionised, so they come under pressure from nearby protons, ions and electrons. Elementary calculations show that the Coulomb repulsion force existing between two protons can be counteracted by extra electrons behind one of the protons. This is expected to occur randomly near the zinc particles and is aided by density fluctuation in the hot ambient plasma. The nuclear strong force between protons can thereby prevail and cause p-p fusion; then the energy release leads to explosive avalanche if the confinement can be maintained for around 50 microseconds. A full theory is not yet necessary because these results are incontrovertible and sufficient for pragmatic development by accomplished teams.

4 Conclusion

Strong explosions have been produced in various hydride+catalyst mixtures by shearing them or ionising them electrically in a compression cell. These astonishing results were consistent, and were attributed to nuclear fusion rather than chemical reactions. For commercial power generation, the fuel could be packed into a simple target and impacted by a fast projectile [3]. Fortunately, these techniques and chemicals are already available and tritium is not involved. No radiation has been detected either.

Energy security is currently an issue of great concern [4]. Climate-change continues to destroy natural ecosystems and property [5]. Prevention will be the least expensive strategy.

Acknowledgements

I would like to thank Imperial College Libraries.

References

1. Wayte R: A Technique for Making Nuclear Fusion in Solids.
J. Condensed Matter Nucl. Sci. 18 (2016) 36-49.

European Patent Specification EP2994916B1.

United States Patent US12221401B2 .

2. Wayte R: A Technique for Making Nuclear Fusion in Solids_More Elements.

www.vixra.org/abs/2504.0019

www.researchgate.net

3. First Light Fusion | Enabling Inertial Fusion Energy | About Us

4. British Energy Security Strategy - GOV.UK

5. [ClimateChange | United Nations](#)